

Noise-Domain Non-Orthogonal Multiple Access

Erkin Yapici, *Graduate Student Member, IEEE*, Yusuf Islam Tek, *Graduate Student Member, IEEE*,
and Ertugrul Basar, *Fellow, IEEE*

Abstract—In this paper, we present noise-domain non-orthogonal multiple access (ND-NOMA), an innovative communication scheme that utilizes the modulation of artificial noise mean and variance to convey information. Distinct from traditional methods such as power-domain non-orthogonal multiple access (PD-NOMA) that heavily relies on successive interference cancellation (SIC), ND-NOMA utilizes the noise domain, considerably reducing power consumption and system complexity. Inspired by noise modulation, ND-NOMA enhances energy efficiency and provides lower bit error probability (BEP), making it highly suitable for next-generation Internet-of-things (IoT) networks. Our theoretical analyses and computer simulations reveal that ND-NOMA can achieve exceptionally low bit error rates in both uplink and downlink scenarios, in the presence of Rician fading channels. The proposed multi-user system is supported by a minimum distance detector for mean detection and a threshold-based detector for variance detection, ensuring robust communication in low-power environments. By leveraging the inherent properties of noise, ND-NOMA offers a promising platform for long-term deployments of low-cost and low-complexity devices.

Index Terms—Noise-domain non-orthogonal multiple access (ND-NOMA), thermal noise communication (TherCom), IoT networks, bit error rate, bit error probability, next-generation communication, multi-user systems.

I. INTRODUCTION

Orthogonal multiple access (OMA) techniques offer advantages such as effective interference management, simplicity of implementation, and fair resource allocation. However, they also present several disadvantages, including reduced efficiency as number of users increases, challenges in dynamic resource allocation, scalability issues in large-scale networks, and limited flexibility due to the need to maintain orthogonality among users [1]–[3]. While OMA is well-suited for current wireless networks, future scenarios with high-density and dynamic demands may benefit from newer techniques like non-orthogonal multiple access (NOMA).

Unlike traditional OMA techniques, where different users are allocated distinct time, frequency, or code resources, NOMA allows multiple users to share the same time and frequency resources simultaneously. This principle is achieved primarily through two main NOMA techniques: power-domain NOMA (PD-NOMA) and code-domain NOMA (CD-NOMA) [4], [5]. PD-NOMA uses different power levels to multiplex users, employing superposition coding at the transmitter and successive interference cancellation (SIC) at the receiver. SIC decodes the strongest signal first, iteratively subtracting it to decode subsequent signals. However, imperfect signal

cancellation can hinder its effectiveness. CD-NOMA multiplexes users in the code domain using techniques like low-density spreading, sparse code multiple access, lattice-partition multiple access, multi-user shared access, and pattern-division multiple access. These techniques separate user signals with distinct code sequences, offering an alternative to PD-NOMA.

However, NOMA systems face several challenges, such as optimizing power allocation to balance energy efficiency and quality-of-service, requiring accurate channel state information (CSI) for effective SIC operation, and managing residual interference from imperfect SIC. Additionally, there are trade-offs between spectral and energy efficiency, receiver design complexities, SIC error propagation, and sensitivity to channel gain measurements [6]. Interference management, integration with carrier aggregation, and addressing security concerns are also critical for NOMA systems [7].

In earlier times, thermal noise modulation (TherMod) was introduced to convey information using thermal noise [8]. This concept recently evolved into schemes that transmit data using parameters like random signal variance. A transceiver architecture later emerged, using either artificially generated or thermal noise sources [9]. Similarly, noise loop modulation had been utilized to deliver artificial noise in a feedback loop between legitimate users, enhancing unconditional security by preventing eavesdropping without requiring knowledge of the eavesdropper's channel [10]. Parallel to these studies, during transmission variance based sampling was also previously used [11]. It has been shown that noise modulation might provide advantages for simplifying the receiver architectures and robustness to certain channel effects and system impairments. This motivates to consider its application in multi-user environments.

In this work, by taking the noise modulation concept one step further, we propose an innovative communication scheme called noise-domain NOMA (ND-NOMA). This scheme utilizes the mean and variance of the artificial noise signals to transmit data. Basically, bits of one user are modulated using the mean of the noise samples, while bits of the other user are modulated using the variance of the noise samples. Since ND-NOMA leverages noise samples, the system does not require processing steps such as time synchronization and equalization for the downlink scenario. Thus, ND-NOMA significantly reduces power consumption and system complexity, making it ideal for the low power consumption requirements of next-generation applications such as Internet-of-things (IoT) networks. Our theoretical analysis and computer simulations demonstrate that ND-NOMA can achieve exceptionally low bit error rate (BER) in both uplink and downlink scenarios. The robust performance of the system is supported by a minimum distance detector for mean detection and a threshold-based

The authors are with the Communications Research and Innovation Laboratory (CoreLab), Department of Electrical and Electronics Engineering, Koç University, Sariyer 34450, Istanbul, Turkey. Email: eyapici19@ku.edu.tr, ytek21@ku.edu.tr, and ebasar@ku.edu.tr

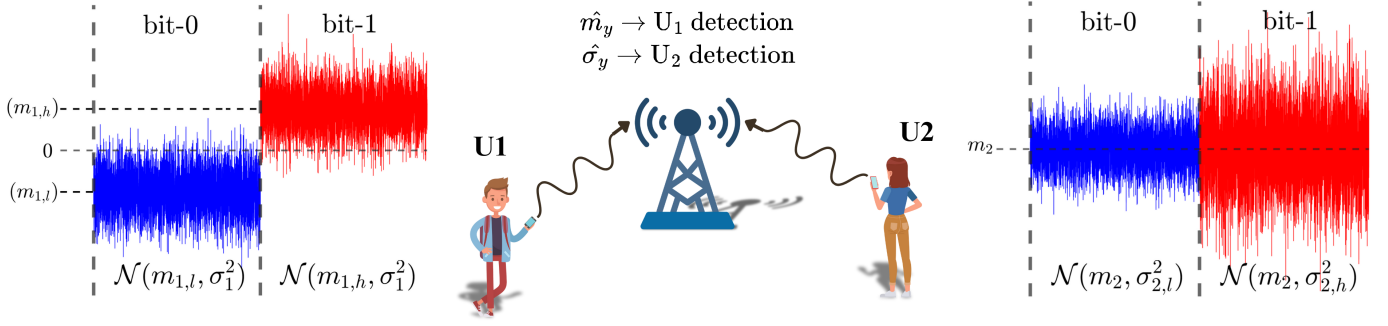


Fig. 1. Uplink ND-NOMA scheme with two users using real Gaussian signals.

detector for variance detection, and ensuring reliable communication even in low-power scenarios. Our findings indicate that ND-NOMA has excellent performance particularly in Rician fading channels and can be utilized for long-term and large-scale deployments of low-cost, low-complex devices.

ND-NOMA is well-suited for integration with Device B types of ambient IoT systems, as highlighted in [12]. Device B, with its limited energy storage and semi-passive operation, aligns with ND-NOMA's low-power and low-complexity demands, essential for sustainable IoT deployments. By utilizing noise mean and variance for data transmission, ND-NOMA reduces the need for power-intensive processes like synchronization, making it ideal for energy-efficient systems. Its robustness in low-power scenarios further enhances the performance of ambient IoT networks, positioning ND-NOMA as a strong contender for next-generation applications. Studies in ISAC show that random waveforms enhance spectral efficiency, complementing ND-NOMA's goals of low-power communication [13]. Moreover, energy harvesting techniques such as SWIPT further support ND-NOMA's energy-efficient design [14], [15].

The fascinating property of Gaussian distribution is that the sum of two independent Gaussian variables remains Gaussian [16]. In ND-NOMA, we exploit this by adding two Gaussian noise signals, each carrying different user information. The resulting signal retains its Gaussian nature, simplifying processing and detection at the receiver. This allows ND-NOMA to efficiently handle multiple signals with minimal error, ideal for low-power IoT networks.

This article is structured as follows. Section II covers uplink ND-NOMA theory and BEP optimization, Section III addresses downlink performance, Section IV presents numerical results, and Section V concludes the paper.

II. UPLINK ND-NOMA: SYSTEM MODEL AND PERFORMANCE ANALYSIS

In this section, we first provide the system model for uplink ND-NOMA for two users and then introduce a general framework to assess the theoretical BEP performance of the two users.

A. System Model

As shown in Fig. 1, in the uplink transmission of two users, one of the users (User 1, U_1) uses the mean of the

transmitted Gaussian samples. In contrast, the other user (User 2, U_2) exploits the variance as in noise modulation schemes. Specifically, denoting the n th noise samples of U_1 and U_2 respectively by s_1^n and s_2^n , for U_1 , the transmission of information bits is accomplished by alternating the mean of the samples between low and high values, that is, for bit-0 and bit-1, we have, $s_1^n \sim \mathcal{N}(m_{1,l}, \sigma_1^2)$ and $s_1^n \sim \mathcal{N}(m_{1,h}, \sigma_1^2)$. As discussed later, we set $m_{1,h} = -m_{1,l}$ for optimum performance. We assume that two users consider N noise samples for each bit.

On the other hand, for U_2 , we apply noise modulation by alternating the noise variance only, and for bit-0 and bit-1, we have $s_2^n \sim \mathcal{N}(m_2, \sigma_{2,l}^2)$ and $s_2^n \sim \mathcal{N}(m_2, \sigma_{2,h}^2)$. At this point, we set the mean of samples to zero, that is, $m_2 = 0$, to minimize the interference to U_1 . This initial model assumes binary-level signaling, while a generalization is subject to further studies.

In this setup, we assume an average transmission power of P for each user, which corresponds to the second moment of the transmitted samples¹: $E[(s_1^n)^2] = E[(s_2^n)^2] = P$, which equals to the sum of squared mean and variance of their samples. In light of this, $P = m_{1,l}^2 + \sigma_1^2$ for U_1 . Here, U_1 dedicates β portion of its available power for the variance of its samples while dedicating a $(1 - \beta)$ portion for the mean, that is, $\sigma_1^2 = \beta P$ and $m_{1,l}^2 = m_{1,h}^2 = (1 - \beta)P$. Since $m_2 = 0$, all power of U_2 is dedicated to the variance of its samples, $P = (\sigma_{2,l}^2 + \sigma_{2,h}^2)/2$.

In what follows, we use the terminology considered in the study of [8] and define $\delta = \sigma_{2,l}^2/\sigma_w^2$ as the ratio of useful and disruptive noise variances. Additionally, α stands for the ratio of high and low variance values for U_2 , that is, $\sigma_{2,h}^2 = \alpha\sigma_{2,l}^2$. Accordingly, we obtain $\eta = \sigma_1^2/\sigma_w^2 = (1 + \alpha)\delta\beta/2$.

In light of the model in Fig. 1, the received n th noise sample at the receiver is expressed as

$$y^n = h_1 s_1^n + h_2 s_2^n + w^n, \quad n = 1, \dots, N. \quad (1)$$

Here, h_1 and h_2 are the complex baseband channel coefficients of the links between U_1 -BS and U_2 -BS, respectively, and $w^n \sim \mathcal{CN}(0, \sigma_w^2)$ is the complex baseband additive white Gaussian noise sample at the BS. Our analysis and computer

¹ Assuming equiprobable U_2 bits, over a long sequence, half of its samples will have $\sigma_{2,l}^2$ variance while the other half having $\sigma_{2,h}^2$. As a request, the second moment of U_2 samples converges to P .

simulations assume either unit-gain Rayleigh or Rician fading models. Accordingly, for Rayleigh fading, we have $h_1, h_2 \sim \mathcal{CN}(0, 1)$ while for Rician fading with K parameter, we have $h_{1,R}, h_{1,I}, h_{2,R}, h_{2,I} \sim \mathcal{N}\left(\sqrt{\frac{K}{2(1+K)}}, \frac{1}{2(1+K)}\right)$. Then, conditioned on channel coefficients, we obtain

$$\begin{aligned} \mathbb{E}[y^n] &= h_1 m_{1,i} \\ \text{VAR}[y^n] &= |h_1|^2 \sigma_1^2 + |h_2|^2 \sigma_{2,k}^2 + \sigma_w^2, \quad i, k \in \{l, h\}. \end{aligned} \quad (2)$$

The task of the BS is to process the received samples of (1) through statistical tests to detect the information bits of both users. The following two subsections present minimum distance-based detection rules for both users and derive their theoretical bit error probability (BEP) performance.

B. Uplink - User 1 Detection

The task of the BS during the detection of U_1 's bit involves calculating the sample mean of the received samples, y^n , $n = 1, \dots, N$, followed by a decision process. In light of this, the sample mean is calculated as

$$\bar{y} = \frac{1}{N} \sum_{n=1}^N y^n, \quad (3)$$

which is complex Gaussian distributed with mean $\mathbb{E}[\bar{y}] = h_1 m_{1,i}$ (unbiased estimate) and $\text{VAR}[\bar{y}] = (|h_1|^2 \sigma_1^2 + |h_2|^2 \sigma_{2,k}^2 + \sigma_w^2)/N$ variance with $i, k \in \{l, h\}$. Based on this, the following binary hypothesis test is considered at the BS to detect U_1 's bit:

$$\hat{b}_1 = \begin{cases} 0, & \text{if } |\bar{y} - h_1 m_{1,l}|^2 < |\bar{y} - h_1 m_{1,h}|^2 \\ 1, & \text{if } |\bar{y} - h_1 m_{1,h}|^2 < |\bar{y} - h_1 m_{1,l}|^2. \end{cases} \quad (4)$$

The above detector is a "minimum distance detector" and considering the complex Gaussian distribution of \bar{y} , it is a *maximum likelihood* one. In light of this and also considering the symmetry for bit-0 and bit-1, conditioned on channel coefficients, the BEP of U_1 becomes

$$P_b = P(|\bar{y} - h_1 m_{1,h}|^2 < |\bar{y} - h_1 m_{1,l}|^2 | b_1 = 0). \quad (5)$$

Expanding the terms in (5) and considering $m_{1,h} = -m_{1,l}$, we obtain

$$P_b = P(4\text{Re}\{\bar{y} h_1^* m_{1,l}\} < 0 | b_1 = 0). \quad (6)$$

Defining the Gaussian distributed random variable $D = \text{Re}\{\bar{y} h_1^* m_{1,l}\}$, we obtain, $P_b = P(D < 0 | b_1 = 0) = Q(m_D/\sigma_D)$, where $\mathbb{E}[D] = m_D$ and $\text{VAR}[D] = \sigma_D^2$ are conditional statistics of D . While m_D can be easily obtained as $m_D = |h_1|^2 m_{1,l}^2$, derivation of σ_D^2 is not straightforward due to correlation of \bar{y}_R and \bar{y}_I . Specifically, we obtain

$$\begin{aligned} \sigma_D^2 &= \text{VAR}[\text{Re}\{(\bar{y}_R + j\bar{y}_I)(h_{1,R} + jh_{1,I})m_{1,l}\}] \\ &= \text{VAR}[m_{1,l}(\bar{y}_R h_{1,R} + \bar{y}_I h_{1,I})] \\ &= m_{1,l}^2 (h_{1,R}^2 \text{VAR}[\bar{y}_R] + h_{1,I}^2 \text{VAR}[\bar{y}_I] \\ &\quad + 2h_{1,R}h_{1,I} \text{COV}(\bar{y}_R, \bar{y}_I)). \end{aligned} \quad (7)$$

Substituting the following variance values in (7) that are obtained after tedious calculations,

$$\begin{aligned} \text{VAR}[\bar{y}_R] &= \frac{1}{N} (h_{1,R}^2 \sigma_1^2 + h_{2,R}^2 \sigma_{2,k}^2 + \sigma_w^2/2) \\ \text{VAR}[\bar{y}_I] &= \frac{1}{N} (h_{1,I}^2 \sigma_1^2 + h_{2,I}^2 \sigma_{2,k}^2 + \sigma_w^2/2) \\ \text{COV}(\bar{y}_R, \bar{y}_I) &= \frac{1}{N} (h_{1,R}h_{1,I} \sigma_1^2 + h_{2,R}h_{2,I} \sigma_{2,k}^2), \end{aligned} \quad (8)$$

BEP of U_1 can be obtained as $P_b = Q(m_D/\sigma_D)$, which is conditioned on h_1, h_2 , and $\sigma_{2,k}^2$. Due to the complexity of the terms inside the Q function, we resort to numerical integration methods over the probabilistic distributions of h_1 and h_2 to derive the unconditional BEP. Specifically, we obtain

$$\bar{P}_b = \iiint P_b f(h_{1,R}) f(h_{1,I}) f(h_{2,R}) f(h_{2,I}) dh_{1,R} dh_{1,I} dh_{2,R} dh_{2,I}, \quad (9)$$

where a further averaging is needed over the two equiprobable values of $\sigma_{2,k}^2$ for $k \in \{l, h\}$. In order to calculate the unconditional BEP, we encountered a highly complex integral that cannot be solved analytically. Consequently, we utilized numerical methods, specifically Monte Carlo integration, to perform the evaluation. The detailed methodology for this approach is provided in Appendix A and is used to calculate the unconditional BEP among the users on both downlink and uplink scenarios.

Finally, we note that, as NoiseMod schemes, conditional BEP is a decaying function of \sqrt{N} (through σ_D^2). Section IV investigates the unconditional BEP over different types of fading channels.

C. Uplink - User 2 Detection

In contrast to U_1 's mean detection problem, the task of the BS is to formulate a variance detection problem to extract U_2 's bits. While we work on a real and positive search space for this problem, complex distributions of y^n and \bar{y} , more importantly, their correlated real and imaginary components, possess a severe challenge on the BEP derivation of U_2 .

In light of this, the sample variance of the received samples is calculated as

$$s_y^2 = \frac{1}{N-1} \sum_{n=1}^N |y^n - \bar{y}|^2. \quad (10)$$

Considering the two possible variance values of y^n , given as $s_0^2 = \sigma_1^2 |h_1|^2 + \sigma_{2,l}^2 |h_2|^2 + \sigma_w^2$ and $s_1^2 = \sigma_1^2 |h_1|^2 + \sigma_{2,h}^2 |h_2|^2 + \sigma_w^2$, further we obtain,

$$\begin{aligned} s_0^2 &= \sigma_w^2 (1 + \eta |h_1|^2 + \delta |h_2|^2) \\ s_1^2 &= \sigma_w^2 (1 + \eta |h_1|^2 + \alpha \delta |h_2|^2). \end{aligned} \quad (11)$$

Here, η , δ , and α are system-related constants defined in Section II.A. Defining a variance threshold as $\gamma = \chi \sigma_w^2$, U_2 detection problem is formulated as

$$\hat{b}_2 = \begin{cases} 0, & \text{if } s_y^2 < \gamma \\ 1, & \text{if } s_y^2 > \gamma, \end{cases} \quad (12)$$

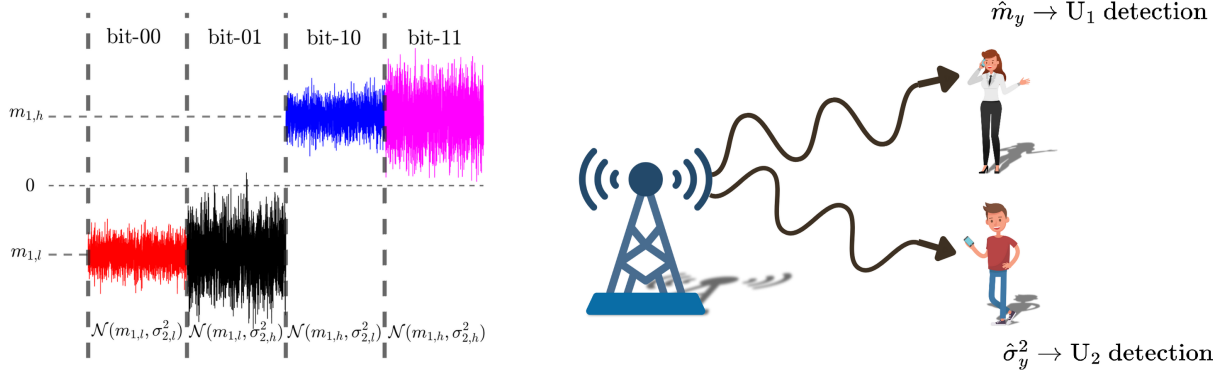


Fig. 2. Downlink ND-NOMA scheme with two users using real Gaussian signals.

Accordingly, BEP of U_2 bits is obtained as

$$P_b = \frac{1}{2} P(s_y^2 > \gamma | b_2 = 0) + \frac{1}{2} P(s_y^2 < \gamma | b_2 = 1). \quad (13)$$

This calculation requires the statistics of s_y^2 , which will be derived next.

At this point, for large N , to simplify the theoretical derivations due to correlated components, we assume $s_y^2 \approx \frac{1}{N-1} \sum_{n=1}^N |y^n - h_{1,l} m_{1,i}|^2$, where \bar{y} is replaced by its mean $E[\bar{y}] = h_{1,l} m_{1,i}$, $i \in \{l, h\}$. Accordingly, (10) can be expressed in the quadratic form of $2N$ real Gaussian random variables:

$$s_y^2 = \frac{1}{N-1} \sum_{n=1}^N (y_R^n - h_{1,R} m_{1,i})^2 + (y_I^n - h_{1,I} m_{1,i})^2 = \mathbf{y}^T \Lambda \mathbf{y}, \quad (14)$$

where $\mathbf{y} \sim \mathcal{N}(\mathbf{0}, \Sigma)$ is a $2N \times 1$ vector with Gaussian distributed elements and Λ is a $2N \times 2N$ diagonal matrix. Here, Σ is a banded covariance matrix, given as

$$\Sigma = \begin{bmatrix} \sigma_R^2 & c & 0 & \dots & 0 \\ c & \sigma_I^2 & 0 & \dots & 0 \\ 0 & 0 & \ddots & & 0 \\ \vdots & \vdots & \dots & 0 & \sigma_R^2 & c \\ 0 & 0 & \dots & 0 & c & \sigma_I^2 \end{bmatrix}_{2N \times 2N} \quad (15)$$

where $\sigma_R^2 = \text{VAR}[y_R^n] = h_{1,R}^2 \sigma_1^2 + h_{2,R}^2 \sigma_{2,k}^2 + \sigma_w^2/2$, $\sigma_I^2 = \text{VAR}[y_I^n] = h_{1,I}^2 \sigma_1^2 + h_{2,I}^2 \sigma_{2,k}^2 + \sigma_w^2/2$, and $c = \text{COV}((y_R^n - h_{1,R} m_{1,i}), (y_I^n - h_{1,I} m_{1,i}))$ for $i, k \in \{l, h\}$ and $n = 1, \dots, N$. After simple manipulations, we obtain $c = h_{1,R} h_{1,I} \sigma_1^2 + h_{2,R} h_{2,I} \sigma_{2,k}^2$.

At this point, interested readers might resort to advanced statistics by considering series expansions for the distribution of Gaussian quadratic forms or advanced mathematical packages on generalized chi-square distributions [17]. To simplify our analysis, we consider the central limit theorem (CLT) and assume that $s_y^2 \sim \mathcal{N}(\mu_s, \sigma_s^2)$ for large enough N .

From [18], we obtain the mean and variance of s_y^2 as

$$\begin{aligned} \mu_s &= \frac{1}{N-1} \text{tr}[\Lambda \Sigma] = \frac{N(\sigma_R^2 + \sigma_I^2)}{N-1} \\ \sigma_s^2 &= \frac{2}{(N-1)^2} \text{tr}[\Lambda \Sigma \Lambda \Sigma] = \frac{2N}{(N-1)^2} (\sigma_R^4 + \sigma_I^4 + 2c^2), \end{aligned} \quad (16)$$

which are consistent with the definition of s_y^2 in (10). Accordingly, BEP is obtained as

$$P_b = \frac{1}{2} Q\left(\frac{\gamma - \mu_s | b_2=0}{\sigma_s | b_2=0}\right) + \frac{1}{2} Q\left(\frac{\mu_s | b_2=1 - \gamma}{\sigma_s | b_2=1}\right) \quad (17)$$

where μ_s and σ_s are conditioned on the transmitted bit through $\sigma_{2,k}^2$. Selecting the threshold for equal bit error probabilities of bit 0 and bit 1 yields

$$\gamma = \frac{\sigma_s | b_2=0 \times \mu_s | b_2=1 + \sigma_s | b_2=1 \times \mu_s | b_2=0}{\sigma_s | b_2=0 + \sigma_s | b_2=1}. \quad (18)$$

Substituting this value in (17) yields the conditional BEP as

$$P_b = Q\left(\frac{\mu_s | b_2=1 - \mu_s | b_2=0}{\sigma_s | b_2=0 + \sigma_s | b_2=1}\right). \quad (19)$$

As U_1 's BEP, for $N \gg 1$, we observe that U_2 's BEP is a decaying function of \sqrt{N} through the σ_s^2 term in the Q function.

Despite its simple detection architecture and our assumptions above, the final result for the BEP is still too complicated for taking an average over channel realizations, and we have to use numerical integration as in (9) to obtain unconditional BEP.

III. DOWNLINK ND-NOMA: SYSTEM MODEL AND PERFORMANCE ANALYSIS

In this section, we emphasize downlink ND-NOMA for two users by defining its system model and then presenting its theoretical BEP performance.

A. System Model

As shown in 2, for the downlink scheme, a composite signal is generated by the BS considering the information bits of two users. Here, we again consider binary modulation for

TABLE I
STATISTICS OF THE TRANSMITTED AND RECEIVED SIGNALS FOR
DOWNLINK ND-NOMA

U_1/U_2 bits	s_{BS}^n	$y_p^n, p \in \{1, 2\}$
00	$\mathcal{N}(m_{1,l}, \sigma_{2,l}^2)$	$\mathcal{CN}(h_p m_{1,l}, h_p ^2 \sigma_{2,l}^2 + \sigma_w^2)$
01	$\mathcal{N}(m_{1,l}, \sigma_{2,h}^2)$	$\mathcal{CN}(h_p m_{1,l}, h_p ^2 \sigma_{2,h}^2 + \sigma_w^2)$
10	$\mathcal{N}(m_{1,h}, \sigma_{2,l}^2)$	$\mathcal{CN}(h_p m_{1,h}, h_p ^2 \sigma_{2,l}^2 + \sigma_w^2)$
11	$\mathcal{N}(m_{1,h}, \sigma_{2,h}^2)$	$\mathcal{CN}(h_p m_{1,h}, h_p ^2 \sigma_{2,h}^2 + \sigma_w^2)$

simplicity. Accordingly, BS's transmitted noise samples follow $s_{BS}^n \sim \mathcal{N}(m_{1,i}, \sigma_{2,k}^2)$ distribution for $i, k \in \{l, h\}$. In other words, the mean of the transmitted signal is dictated by U_1 's bit while its variance is determined according to U_2 's bit. In this case, the received signals at two users are given by

$$\begin{aligned} y_1^n &= h_1 s_{BS}^n + w_1^n \\ y_2^n &= h_2 s_{BS}^n + w_2^n, \end{aligned} \quad (20)$$

for $n = 1, \dots, N$. Here, h_1 and h_2 stand for the downlink channel fading coefficients between the BS and users, and w_1^n and w_2^n are AWGN samples at users with $\mathcal{CN}(0, \sigma_w^2)$ distribution. Specifically, Table I lists the distribution of the transmitted and received signals at all terminals depending on four user bit combinations, 00, 01, 10, and 11, where the first and second bits respectively stand for U_1 and U_2 bits for a given bit duration.

Here, we assume that the total transmission power is fixed to P , that is, $E[(s_{BS}^n)^2] = P$. Similar to the β parameter of the uplink scheme, we define a new parameter, ψ , as the portion of U_1 's allocated power, that is, $m_{1,l}^2 = m_{1,h}^2 = \psi P$ (dc power of the transmitted signal). Accordingly, for U_2 , we have $(\sigma_{2,l}^2 + \sigma_{2,h}^2)/2 = (1 - \psi)P$ (ac power of the transmitted signal). We again consider $m_{1,h} = -m_{1,l}$ and $\sigma_{2,h}^2 = \alpha \sigma_{2,l}^2$. Later, we will show that the performance of U_1 and U_2 highly depends on the selection of ψ parameter.

Since the users' signals do not overlap as in the uplink scheme, the detection model of the downlink system is much simpler, and there is no interaction among user signals. Furthermore, there is no need for successive interference cancellation and error propagation issues as in the downlink PD-NOMA scheme. In what follows, we provide detector architectures for both users.

B. Downlink - User 1 Detection

The receiver architecture of the downlink scheme for U_1 is very similar to that of the uplink scheme, and the BEP can be evaluated by simple modifications. Specifically, U_1 calculates the sample mean of its received samples as $\bar{y}_1 = \frac{1}{N} \sum_{n=1}^N y_1^n$, which is also Gaussian distributed with $E[\bar{y}_1] = h_1 m_{1,i}$ and $\text{VAR}[\bar{y}_1] = (|h_1|^2 \sigma_{2,k}^2 + \sigma_w^2)/N$ for $i, k \in \{l, h\}$. Accordingly, the minimum distance detector is formulated as

$$\hat{b}_1 = \begin{cases} 0, & \text{if } |\bar{y}_1 - h_1 m_{1,l}|^2 < |\bar{y}_1 - h_1 m_{1,h}|^2 \\ 1, & \text{if } |\bar{y}_1 - h_1 m_{1,h}|^2 < |\bar{y}_1 - h_1 m_{1,l}|^2. \end{cases} \quad (21)$$

Similar to the uplink scheme's BEP in (5), BEP for this case is obtained as

$$\begin{aligned} P_b &= P(|\bar{y}_1 - h_1 m_{1,h}|^2 < |\bar{y}_1 - h_1 m_{1,l}|^2 | b_1 = 0) \\ &= P(\text{Re}\{\bar{y}_1 h_1^* m_{1,l}\} < 0 | b_1 = 0) \\ &= P(D < 0 | b_1 = 0) = Q(m_D / \sigma_D). \end{aligned} \quad (22)$$

Here, Gaussian distributed variable D has the following statistics: $m_D = |h_1|^2 m_{1,l}^2$ and $\sigma_D^2 = m_{1,l}^2 (h_{1,R}^2 \text{VAR}[\bar{y}_{1,R}] + h_{1,I}^2 \text{VAR}[\bar{y}_{1,I}] + 2h_{1,R}h_{1,I} \text{COV}(\bar{y}_{1,R}, \bar{y}_{1,I}))$. With simple manipulations, variance values are obtained as

$$\begin{aligned} \text{VAR}[\bar{y}_{1,R}] &= \frac{1}{N} (h_{1,R}^2 \sigma_{2,k}^2 + \sigma_w^2/2) \\ \text{VAR}[\bar{y}_{1,I}] &= \frac{1}{N} (h_{1,I}^2 \sigma_{2,k}^2 + \sigma_w^2/2) \\ \text{COV}(\bar{y}_{1,R}, \bar{y}_{1,I}) &= \frac{1}{N} h_{1,R} h_{1,I} \sigma_{2,k}^2. \end{aligned} \quad (23)$$

Conditional BEP is obtained by substituting these values in σ_D^2 first and then considering (22).

C. Downlink - User 2 Detection

Finally, this subsection investigates the receiver architecture and performance of U_2 for the downlink scheme. Fortunately, the same analytical framework of Section II.C can be considered here for slight modifications.

For U_2 's variance detection in the downlink scheme, the sample variance is obtained as

$$s_{y_2}^2 = \frac{1}{N-1} \sum_{n=1}^N |y_2^n - \bar{y}_2|^2 \quad (24)$$

where \bar{y}_2 is the sample mean for the samples of U_2 . Here, in a similar manner to uplink detection, we define a variance threshold as $\gamma = \chi \sigma_w^2$ and formulate U_2 detection problem as

$$\hat{b}_2 = \begin{cases} 0, & \text{if } s_{y_2}^2 < \gamma \\ 1, & \text{if } s_{y_2}^2 > \gamma. \end{cases} \quad (25)$$

In light of this, BEP of the U_2 bit is obtained as

$$P_b = \frac{1}{2} P(s_{y_2}^2 > \gamma | b_2 = 0) + \frac{1}{2} P(s_{y_2}^2 < \gamma | b_2 = 1). \quad (26)$$

To use the same analysis of Section III.C, we again resort to the strong law of large numbers by assuming $s_{y_2}^2 \approx \frac{1}{N-1} \sum_{n=1}^N |y_2^n - h_2 m_{1,i}|^2$. Expressing, this new $s_{y_2}^2$ in the quadratic form of $2N$ real Gaussian random variables as $s_{y_2}^2 = \mathbf{y}^T \Lambda \mathbf{y}$, where \mathbf{y} and Λ are as defined in (14), we obtain the same banded covariance matrix of (15) with the following updated parameters:

$$\begin{aligned} \sigma_R^2 &= \text{VAR}[y_{2,R}^n] = h_{2,R}^2 \sigma_{2,k}^2 + \sigma_w^2/2 \\ \sigma_I^2 &= \text{VAR}[y_{2,I}^n] = h_{2,I}^2 \sigma_{2,k}^2 + \sigma_w^2/2 \\ c &= \text{COV}((y_{2,R}^n - h_{2,R} m_{1,i}), (y_{2,I}^n - h_{2,I} m_{1,i})) \\ &= h_{2,R} h_{2,I} \sigma_{2,k}^2. \end{aligned} \quad (27)$$

Considering CLT and substituting the new values of (27) first in (16), then updating (17)-(19) accordingly, conditional BEP is obtained.

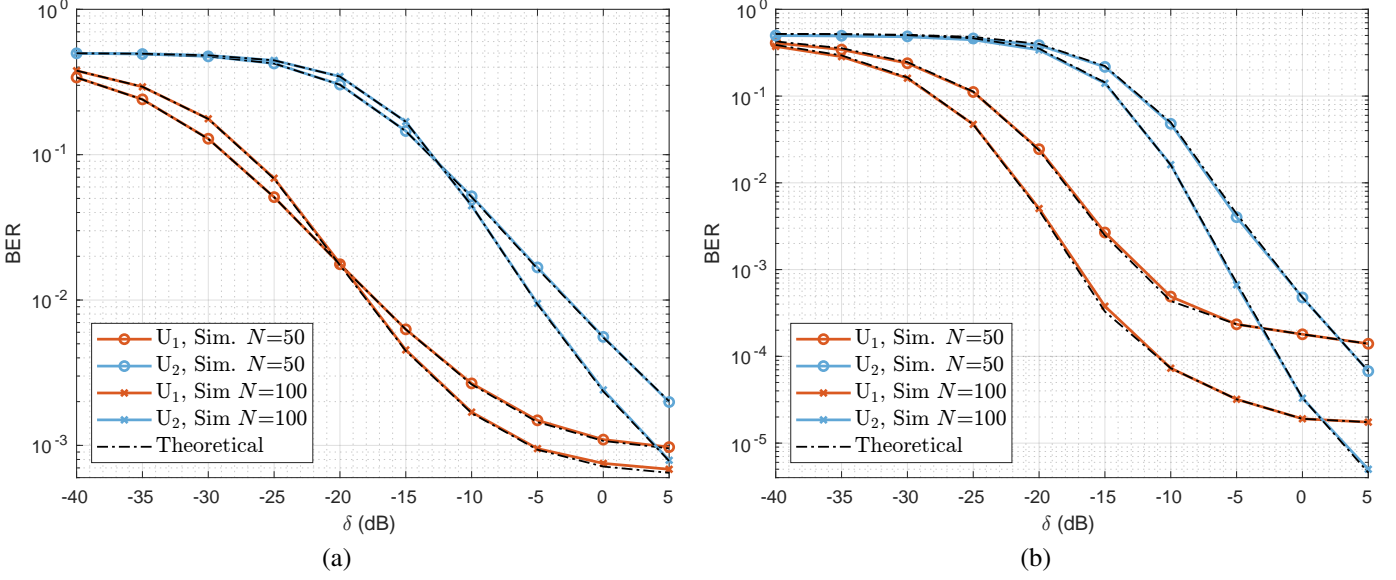


Fig. 3. Theoretical BEP and simulated BER for uplink ND-NOMA versus $\delta = \sigma_l^2 / \sigma_w^2$, with Rician K -factor values of (a) $K = 5$ and (b) $K = 10$ dB

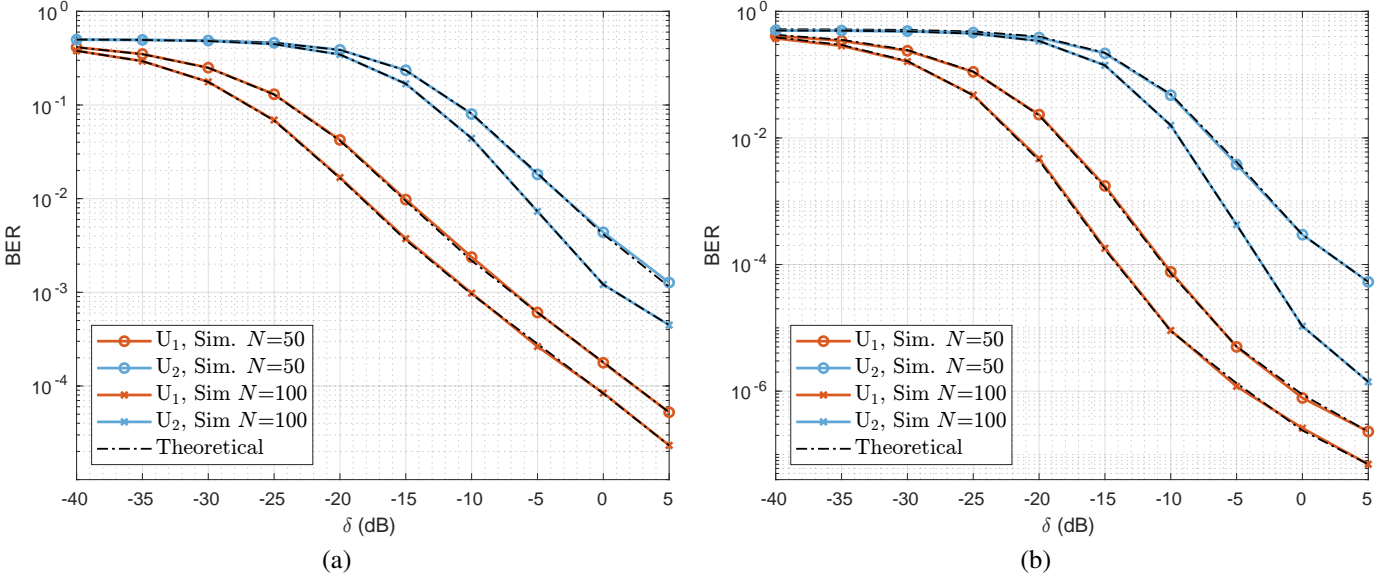


Fig. 4. Theoretical BEP and simulated BER for downlink ND-NOMA versus $\delta = \sigma_l^2 / \sigma_w^2$, with Rician K -factor values of (a) $K = 5$ and (b) $K = 10$ dB

IV. NUMERICAL RESULTS

In this section, we analyze the bit error rate (BER) performance of the proposed ND-NOMA system in both uplink and downlink scenarios. In our analysis, the channel coefficients are modeled as if their envelopes are Rician distributed, $h_{1,R}, h_{1,I}, h_{2,R}, h_{2,I} \sim \mathcal{N}\left(\sqrt{\frac{K}{2(1+K)}}, \frac{1}{2(1+K)}\right)$, where K being the Rician factor. This choice of distribution reflects the pres-

ence of a line-of-sight component along with multipath effects, capturing the realistic propagation conditions for the wireless channels considered in our study. Moreover, we employed Monte Carlo integration method, as described in Appendix A, to compute the unconditional BEP for uplink and downlink scenarios so as to verify our computer simulation results. The simulation parameters are outlined in Table II.

A. Uplink Scenario

Figs. 3(a) and 3(b) illustrate the BER performance of U_1 and U_2 for $K \in \{5, 10\}$ respectively where our theoretical derivations verify our simulation results. Herein the increase in the Rician K -factor improves the BER performance of the proposed ND-NOMA system. This enhancement is attributed to the stronger line-of-sight component in the Rician channel, which enhances detection performance for both U_1 and U_2 in the uplink scenario. In Fig. 3(b) where $K = 10$, U_1 exhibits better BER performance compared to U_2 , since U_1 's detection

TABLE II
SIMULATION PARAMETERS

Parameter	Value	Reference
K_{dB}	5, 10	-
N	50, 100	[8]
δ_{dB}	[-40, 5]	-
α	10	[8]
P_{dBm}	30	-
β	1/100	-

mechanism leverages the mean of the transmitted Gaussian samples, which is more resilient to noise variations compared to U_2 's variance-based detection in our scenario.

The impact of δ on BER is also critical in the uplink scenario. In Figs. 3 and 4, increasing δ which represents the higher ratio of useful to disruptive noise variances, results in improved BER performance as depicted in Figs. 3(a) and 3(b). However in Fig. 3(b), after the δ value of -5 , BER saturates where $N = 50$ for U_1 , since there is an interference between the users. This trend is evident in Figs. 3(a) and 3(b), where higher δ values correlate with improved BER performance. The ability of ND-NOMA to maintain low BER even in scenarios with significant noise variance is demonstrated, indicating its effectiveness in environments with varying noise conditions. It is worth noting that the users of ND-NOMA are not interference-free; nevertheless, its unique nature allows the BS to distinguish user signals without SIC.

Furthermore, another important parameter that significantly effects the BER performance of the proposed ND-NOMA system is the number of the noise samples per bit (N) which stands for the number of samples that are taken to estimate mean for U_1 and estimate the variance for U_2 . As it can be seen in Figs. 3(a) and 3(b), increasing N boosts the performance of the system's uplink scenario. Our findings also underscores the importance of sample size N in reducing BER, highlighting that transition from N being 50 to 100 sample size allow better estimation accuracy of the Gaussian noise parameters, thus minimizing the impact of noise as well as improving overall detection performance.

B. Downlink Scenario

As in the uplink scenario; the downlink scenario's simulation results coincide with our theoretical derivations, in Figs. 4(a) and 4(b), demonstrating the system's reliability even in the high disruptive noise conditions. As expected, the increase in δ as well as K enhances the BER performance of the proposed system in downlink scenario for U_1 and U_2 . Increasing δ as well as N and K improves the system performance. Different from the uplink scenario where $K = 10$, BER performance of ND-NOMA system of U_1 do not saturate after a specific δ value since there is no interference.

We note that the impact of the sample size N on the BER in the downlink scenario is significant. As N increases, the BER decreases for both U_1 and U_2 . This is due to the fact that larger sample sizes allow for better averaging of the noise parameters, which are supported by a minimum distance detector for mean detection at U_1 and a threshold-based detector for variance detection at U_2 , which improves the accuracy of related parameters. Consequently, the ND-NOMA system achieves lower BER with higher N , demonstrating its efficiency and reliability in maintaining high-quality communication in downlink scenarios.

Comparing Fig. 3(b) with Fig. 4(b), where uplink and downlink scenarios are considered respectively, the BER performance of U_2 exhibits similar results for both scenarios. However; in downlink scenario, two bits are transmitted unlike the uplink scenario where one bit of information is conveyed

at every transmission instant. Furthermore, U_1 BER gets saturated since there is an interference in the uplink scenario; however in the downlink scenario since we assume that U_1 signal does not interfere with U_2 signal, its performance does not reach saturation. Additionally, we have presented OMA-NoiseMod scenario in the following subsection, to prevent interference between users.

C. Comparison with OMA-NoiseMod Scenario

In scenarios where two users communicate simultaneously over N noise samples in uplink/downlink, the communication can be divided into two equal parts, $N/2 - N/2$, allowing classic NoiseMod communication without interference. This scheme can be referred to as OMA-NoiseMod. Figs. 5(a) and 5(b) illustrate the comparative BER performance of ND-NOMA and the OMA-NoiseMod scenario for both uplink and downlink transmissions. As shown in Fig. 5(a), ND-NOMA outperforms OMA-NoiseMod in terms of BER under the same conditions, particularly as the Rician K -factor and δ increase.

In the higher Rician K -factor scenario ($K = 10$), as shown in the Fig. 5(b), ND-NOMA continues to exhibit superior BER performance compared to OMA-NoiseMod. The key advantage of ND-NOMA over OMA-NoiseMod lies in its ability to manage user interference through the simultaneous transmission of data. The results clearly show that with an increased number of noise samples (N) and higher Rician K -factors, ND-NOMA achieves lower BER compared to OMA-NoiseMod. This makes ND-NOMA a more efficient and reliable communication scheme.

In the OMA-NoiseMod scenario, both U_1 and U_2 experience the same BER performance because the communication process is divided into non-overlapping time slots or frequency bands, ensuring that both users have identical conditions for transmitting and receiving data. This means there is no interference between the users, and both experience the same signal quality and noise conditions, leading to identical BER outcomes. This explains the reason why their performances are the same in the OMA-NoiseMod scheme.

V. CONCLUSION

In this paper, we have introduced ND-NOMA, an innovative communication scheme that leverages noise variance and mean to transmit data. ND-NOMA significantly reduces power consumption and system complexity by utilizing noise parameters, making it a promising solution for next-generation IoT networks. Through theoretical analysis and simulations, we have demonstrated that ND-NOMA achieves low bit error rates in both uplink and downlink scenarios, outperforming traditional OMA-NoiseMod in spectral efficiency and interference management. The ND-NOMA system employs a minimum distance detector for mean detection and a threshold-based detector for variance detection, ensuring reliable performance even in low-power environments. The results indicate that ND-NOMA's ability to handle high-density device deployments and maintain low BER under varying noise conditions makes it ideal for energy-efficient communications, particularly for

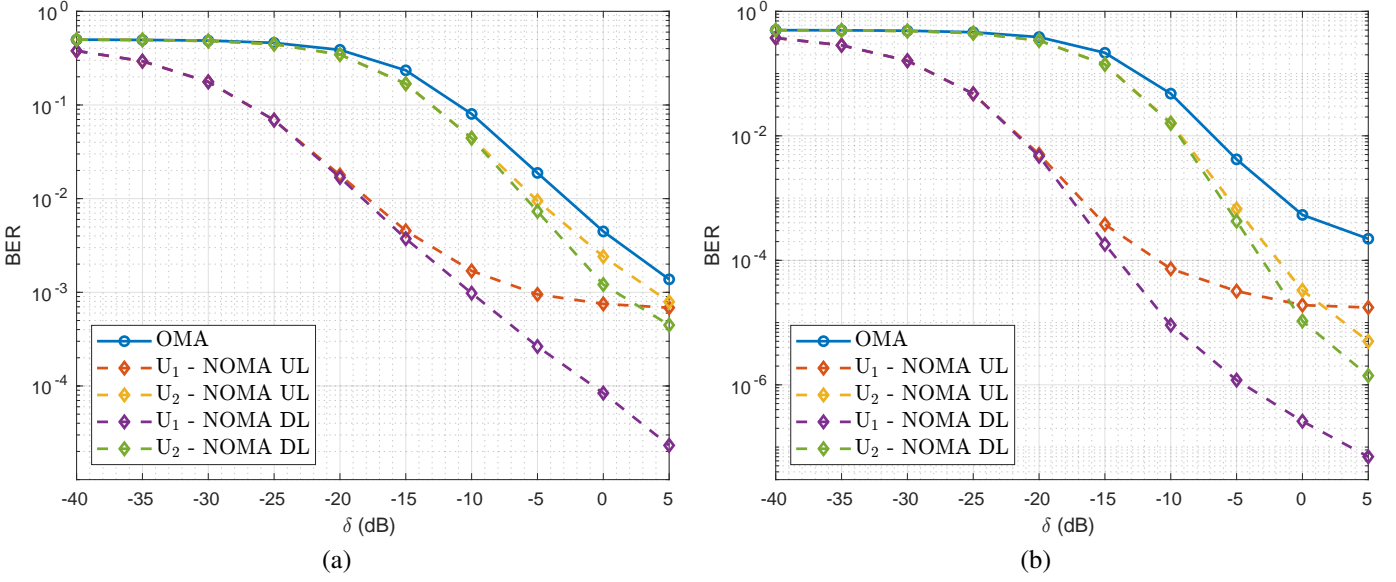


Fig. 5. Comparative BER performance of OMA-NoiseMod and ND-NOMA (uplink and downlink) with respect to δ , with Rician K -factor values of (a) $K = 5$ and (b) $K = 10$ dB

battery-operated and energy-harvesting devices. Its adaptability to diverse noise profiles further enhances its potential for widespread adoption. Future research could explore further optimization of ND-NOMA, such as utilizing noise correlation to enhance performance and robustness.

APPENDIX A MONTE CARLO INTEGRATION METHOD

Monte Carlo integration is a powerful technique for numerically estimating integrals, particularly in high-dimensional spaces or when the integrand has a complex form. In this appendix, we have addressed the problem of unconditional BEP integrals mentioned in previous sections. As an initial step, we can rewrite (9) as

$$\bar{P}_b = \int_V g(h_{1,R}, h_{1,I}, h_{2,R}, h_{2,I}) d\hat{h}, \quad (28)$$

where

$$g(h_{1,R}, h_{1,I}, h_{2,R}, h_{2,I}) = P_b f(h_{1,R}) f(h_{1,I}) f(h_{2,R}) f(h_{2,I})$$

and $d\hat{h} = dh_{1,R} dh_{1,I} dh_{2,R} dh_{2,I}$. Here, V is the whole integration volume. Then, we will utilize importance sampling to compute the integral efficiently. We choose an appropriate joint PDF $z(h_{1,R}, h_{1,I}, h_{2,R}, h_{2,I})$ that matches the form of the integrand as

$$z(h_{1,R}, h_{1,I}, h_{2,R}, h_{2,I}) = z(h_{1,R}) z(h_{1,I}) z(h_{2,R}) z(h_{2,I}), \quad (29)$$

where $z(\cdot)$ denotes the sampling function in the integral volume V ($z > 0$, $\int_V f_n dV = 1$). Specifically, $z(\cdot)$ represents a PDF characterized by the same mean and variance as the PDFs of channel gains $f(\cdot)$, as described in (9). Incorporating this expression, (28) can be reformulated as

$$\bar{P}_b = \int_V \frac{g(h_{1,R}, h_{1,I}, h_{2,R}, h_{2,I}) z(h_{1,R}, h_{1,I}, h_{2,R}, h_{2,I})}{z(h_{1,R}, h_{1,I}, h_{2,R}, h_{2,I})} d\hat{h} \quad (30)$$

Afterwards, we generate J random points for all integral variables from corresponding sampling functions as $\{\mathbf{h}^{(1)}, \mathbf{h}^{(2)}, \dots, \mathbf{h}^{(J)}\}$ where $\mathbf{h}^{(j)} = [h_{1,R}^{(j)}, h_{1,I}^{(j)}, h_{2,R}^{(j)}, h_{2,I}^{(j)}]$ for $j = 1, 2, \dots, J$. Then the importance weights are calculated as follows

$$w(\mathbf{h}^{(j)}) = \frac{g(h_{1,R}^{(j)}, h_{1,I}^{(j)}, h_{2,R}^{(j)}, h_{2,I}^{(j)}) z(h_{1,R}^{(j)}, h_{1,I}^{(j)}, h_{2,R}^{(j)}, h_{2,I}^{(j)})}{z(h_{1,R}^{(j)}, h_{1,I}^{(j)}, h_{2,R}^{(j)}, h_{2,I}^{(j)})}. \quad (31)$$

The integral is estimated using the average of these weights as expressed below: [19]

$$\bar{P}_b = \frac{1}{J} \sum_{j=1}^J w(\mathbf{h}^{(j)}). \quad (32)$$

For unconditional BEP curves, $J = 10^6$ random sample points are used for all integral estimations.

REFERENCES

- [1] L. Dai, B. Wang, Z. Ding, Z. Wang, S. Chen, and L. Hanzo, "A survey of non-orthogonal multiple access for 5G," *IEEE Commun. Surv. Tutor.*, vol. 20, no. 3, pp. 2294–2323, 3rd Quart. 2018.
- [2] B. Zheng, Q. Wu, and R. Zhang, "Intelligent reflecting surface-assisted multiple access with user pairing: NOMA or OMA?" *IEEE Commun. Lett.*, vol. 24, no. 4, pp. 753–757, Apr. 2020.
- [3] J. Ghosh, I.-H. Ra, S. Singh, H. Hacı, K. A. Al-Utaibi, and S. M. Sait, "On the comparison of optimal NOMA and OMA in a paradigm shift of emerging technologies," *IEEE Access*, vol. 10, pp. 11 616–11 632, Jan. 2022.
- [4] S. M. R. Islam, N. Avazov, O. A. Dobre, and K.-S. Kwak, "Power-domain non-orthogonal multiple access (NOMA) in 5G systems: Potentials and challenges," *IEEE Commun. Surveys Tuts.*, vol. 19, no. 2, pp. 721–742, 2nd Quart. 2017.
- [5] X. Dai, Z. Zhang, B. Bai, S. Chen, and S. Sun, "Pattern division multiple access: A new multiple access technology for 5G," *IEEE Wireless Commun.*, vol. 25, no. 2, pp. 54–60, Apr. 2018.
- [6] B. Makki, K. Chitti, A. Behravan, and M. S. Alouini, "A survey of NOMA: Current status and open research challenges," *IEEE Open J. Commun. Soc.*, vol. 1, pp. 179–189, Jan. 2020.
- [7] G. N. Tran, S. Q. Nguyen, M. T. Nguyen, and S. Kim, "Optimal power allocation for non-orthogonal multiple access visible light communications with short packet and imperfect channel information," in *Int. Conf. Adv. Technol. Commun. (ATC)*, Oct. 2022, pp. 234–238.

- [8] E. Basar, "Communication by means of thermal noise: Towards networks with extremely low power consumption," *IEEE Trans. Wirel. Commun.*, vol. 71, no. 2, pp. 688–699, Feb. 2023.
- [9] —, "Noise modulation," *IEEE Wirel. Commun. Lett.*, vol. 13, no. 3, pp. 844–848, Mar. 2024.
- [10] L. Mucchi, S. Caputo, P. Marcocci, G. Chisci, L. Ronga, and E. Panayirci, "Security and reliability performance of noise-loop modulation: Theoretical analysis and experimentation," *IEEE Trans. Veh. Technol.*, vol. 71, no. 6, pp. 6335–6350, Jun. 2022.
- [11] S. Sigg, P. Jakimovski, and M. Beigl, "Calculation of functions on the RF-channel for IoT," in *Proc. IEEE Int. Conf. Internet Things*, Oct. 2012, pp. 107–113.
- [12] M. M. Butt, N. R. Mangalvedhe, N. K. Pratas, J. Harrebek, J. Kimionis, M. Tayyab, O.-E. Barbu, R. Ratasuk, and B. Vejlgaard, "Ambient IoT: A missing link in 3GPP IoT devices landscape," *IEEE Internet Things Mag.*, vol. 7, no. 2, pp. 85–92, Mar. 2024.
- [13] V. Koivunen, M. F. Keskin, H. Wymeersch, M. Valkama, and N. González-Prelcic, "Multicarrier ISAC: Advances in waveform design, signal processing and learning under non-idealities," *arXiv preprint arXiv:2406.18476*, 2024.
- [14] C. Song, C. Ling, J. Park, and B. Clerckx, "MIMO broadcasting for simultaneous wireless information and power transfer: Weighted MMSE approaches," in *2014 IEEE Globecom Workshops, GC Wkshps 2014*, vol. 12, no. 5. IEEE, Dec. 2014, pp. 1151–1156.
- [15] N. Ashraf, S. A. Sheikh, S. A. Khan, I. Shaye, and M. Jalal, "Simultaneous wireless information and power transfer with cooperative relaying for next-generation wireless networks: A review," *IEEE Access*, vol. 9, pp. 71 482–71 504, May 2021.
- [16] Z. Ding, Z. Yang, P. Fan, and H. V. Poor, "On the performance of non-orthogonal multiple access in 5G systems with randomly deployed users," *IEEE Signal Process. Lett.*, vol. 21, no. 12, pp. 1501–1505, Dec. 2014.
- [17] A. Mathai and S. B. Provost, *Quadratic Forms in Random Variables: Theory and Applications*. New York, NY, USA: Marcel Dekker, 1992.
- [18] M. Paoletta, *Linear Models and Time-Series Analysis: Regression, ANOVA, ARMA and GARCH*. New York, NY, USA: Wiley, 2018.
- [19] R. Yuan, J. Ma, P. Su, Y. Dong, and J. Cheng, "Monte-Carlo integration models for multiple scattering based optical wireless communication," *IEEE Trans. Commun.*, vol. 68, no. 1, pp. 334–348, Jan. 2020.